

OAK RIDGE NATIONAL LABORATORY LIBRARIES



3 4456 0548271 4

CENTRAL RESEARCH LIBRARY  
DOCUMENT COLLECTION

ORNL-3815  
UC-22 - Isotope Separation  
TID-4500 (41st ed.)

REVIEW OF ORNL THERMAL DIFFUSION PROGRAM

JANUARY - DECEMBER 1964

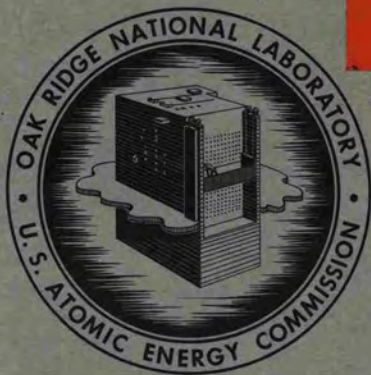
T. A. Butler  
W. R. Rathkamp  
H. B. Greene

CENTRAL RESEARCH LIBRARY  
DOCUMENT COLLECTION

**LIBRARY LOAN COPY**

**DO NOT TRANSFER TO ANOTHER PERSON**

If you wish someone else to see this  
document, send in name with document  
and the library will arrange a loan.



**OAK RIDGE NATIONAL LABORATORY**

operated by

**UNION CARBIDE CORPORATION**

for the

**U.S. ATOMIC ENERGY COMMISSION**

Printed in USA. Price \$2.00. Available from the Clearinghouse for Federal  
Scientific and Technical Information, National Bureau of Standards,  
U.S. Department of Commerce, Springfield, Virginia

LEGAL NOTICE

This report was prepared as an account of Government sponsored work. Neither the United States, nor the Commission, nor any person acting on behalf of the Commission:

- A. Makes any warranty or representation, expressed or implied, with respect to the accuracy, completeness, or usefulness of the information contained in this report, or that the use of any information, apparatus, method, or process disclosed in this report may not infringe privately owned rights; or
- B. Assumes any liabilities with respect to the use of, or for damages resulting from the use of any information, apparatus, method, or process disclosed in this report.

As used in the above, "person acting on behalf of the Commission" includes any employee or contractor of the Commission, or employee of such contractor, to the extent that such employee or contractor of the Commission, or employee of such contractor prepares, disseminates, or provides access to, any information pursuant to his employment or contract with the Commission, or his employment with such contractor.

ORNL-3815

Contract No. W-7405-eng-26

ISOTOPES DEVELOPMENT CENTER

REVIEW OF ORNL THERMAL DIFFUSION PROGRAM

JANUARY-DECEMBER 1964

T. A. Butler  
W. R. Rathkamp  
H. B. Greene

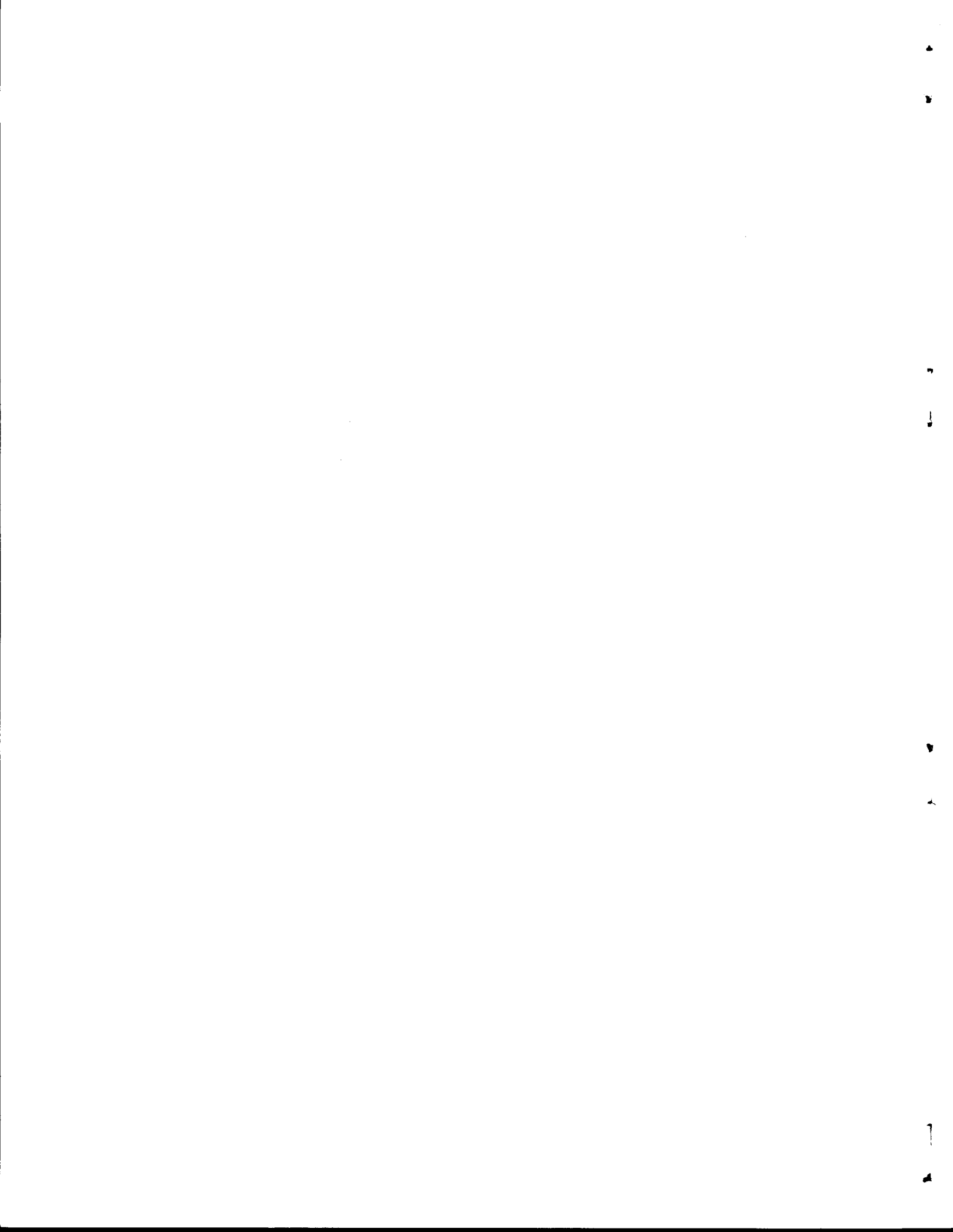
Isotopes Division

JUNE 1965

OAK RIDGE NATIONAL LABORATORY  
Oak Ridge, Tennessee  
operated by  
UNION CARBIDE CORPORATION  
for the  
U.S. ATOMIC ENERGY COMMISSION

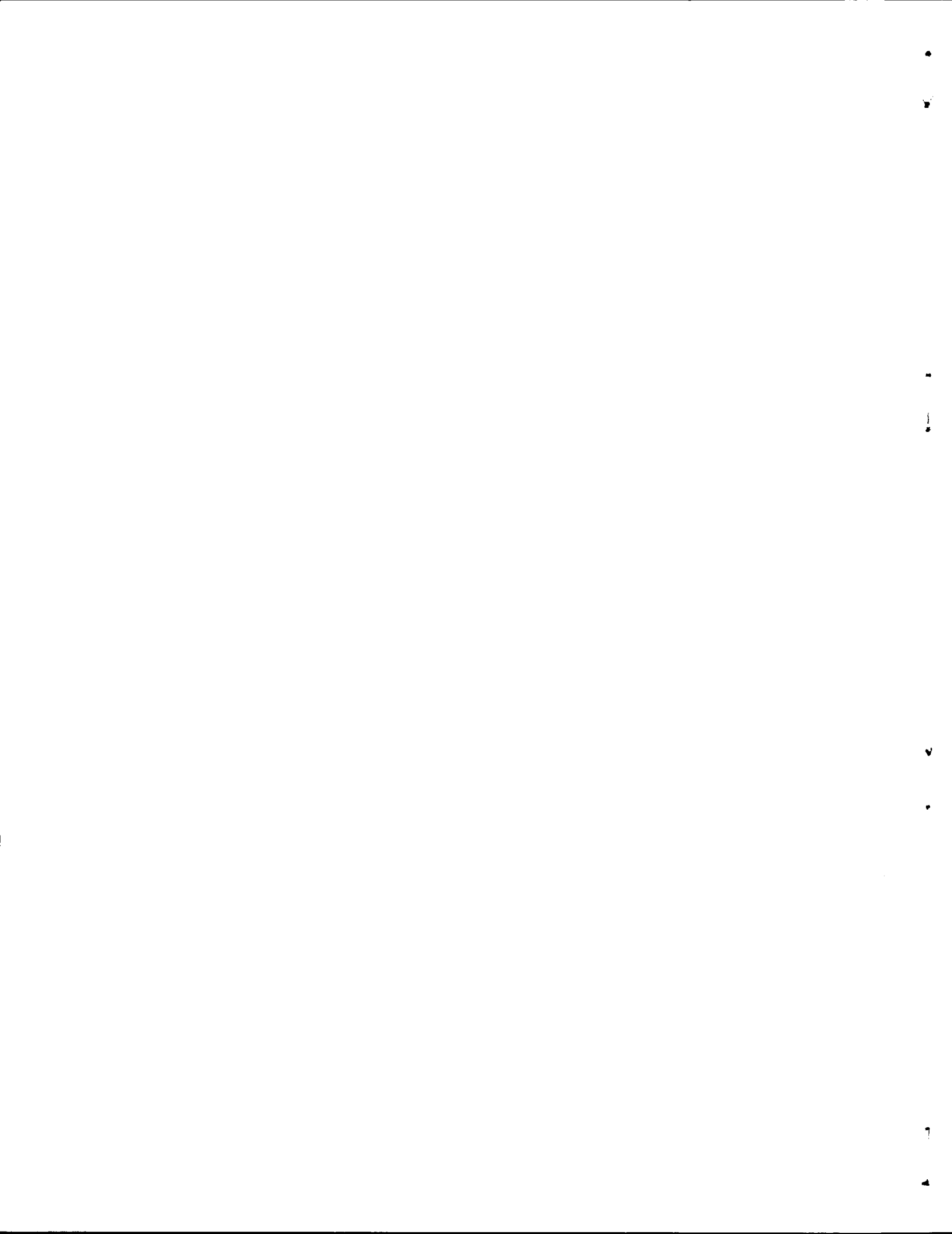


3 4456 0548271 4



CONTENTS

	Page
Abstract . . . . .	1
Theoretical Developments . . . . .	1
Heat Losses . . . . .	1
Pressure at Maximum Separation . . . . .	5
Separation Factor Relationships . . . . .	8
Preenrichment of Feed Material . . . . .	12
Operations and Product Enrichments . . . . .	15
Neon . . . . .	15
Argon . . . . .	17
Krypton . . . . .	19
Xenon . . . . .	21
Product Enrichments . . . . .	21



REVIEW OF ORNL THERMAL DIFFUSION PROGRAMJANUARY-DECEMBER 1964

T. A. Butler, W. R. Rathkamp, H. B. Greene

## ABSTRACT

This review of the activities of the ORNL Thermal Diffusion Program for 1964 includes column operation, methods of increasing the feasibility of isotope separation of inert gases by thermal diffusion, and product enrichments.

The past year's efforts were concentrated on the separation and enrichment of particular isotopes of the inert gases — neon, argon, krypton, and xenon. Chrome-plated columns to minimize heat losses due to radiation from the heaters and conduction through specially designed spacers holding the heating element and preenrichment of feed material were investigated through theoretical developments. Feasibility of these methods was tested and compared to theoretical evaluations by data obtained from actual operating conditions.

---

THEORETICAL DEVELOPMENTSHeat Losses

Heat is removed in four ways from the heating element in a thermal diffusion column: by radiation from the heater, by convection currents in the gas, by conduction through the gas, and by conduction through the spacers between the heater and the cold wall and lengthwise through the heater sheath to the cold jacket end fittings.

Convection and conduction through the gas are essential for the operation of a thermal diffusion column, but if heat loss via radiation or direct conduction through the spacers can be decreased, the over-all economy of operation will increase. Theoretical and experimental investigations of heater temperature and various modes of heat transfer to the cold wall were undertaken to better understand column operation and to increase the efficiency and economy of isotope separation by thermal diffusion.

The amount of heat radiated from the heater and the amount conducted through the spacers and sheath can be determined from power input and heater sheath temperature with an evacuated column (no heat loss due to convection or

conduction through the gas is possible). The power input, in watts, is given by Eq. 1,

$$Q = \text{conduction and radiation} = A(T_2 - T_1) + B(T_2^4 - T_1^4) , \quad (1)$$

where

- $T_2$  = heater sheath temperature, °K,
- $T_1$  = cold wall temperature, °K,
- A = constant determined by conduction factors, and
- B = constant determined by radiation factors.

Dividing by the temperature difference, Eq. 2 is obtained,

$$Q/(T_2 - T_1) = B(T_2^2 + T_1^2)(T_2 + T_1) + A . \quad (2)$$

When the ratio of power input to the temperature difference is plotted against the function,  $(T_2^2 + T_1^2)(T_2 + T_1)$ , a straight line (Fig. 1) is obtained whose slope is equal to B and whose ordinate intercept is equal to A; data of power input and the corresponding temperatures were taken with the column evacuated. Equations 3 and 4 were derived for heat losses by radiation,  $q_r$ , and direct conduction,  $q_{dc}$ , after A and B were evaluated,

$$q_r = 0.21 \times 10^{-8} (T_2^4 - T_1^4) , \quad (3)$$

$$q_{dc} = 0.29 (T_2 - T_1) . \quad (4)$$

Heat is transferred by gas conduction (in cal/sec) between two coaxial cylinders as given by Eq. 5,

$$q_{gc} = \frac{2\pi k(T_2 - T_1)L}{\ln(r_1/r_2)} , \quad (5)$$

where

- L = length of heater, cm,
- $r_1$  = cold wall radius,
- $r_2$  = heater radius, and
- k = thermal conductivity, cal/sec.cm.°K.

For L = 70 in.,  $r_1 = 0.688$  in.,  $r_2 = 0.440$  in., and  $T_1 = 300^\circ\text{K}$ ,  $q_{gc}$  converted to watts by the factor  $4.18 \text{ watts} = 1 \text{ cal/sec}$  is given by Eq. 6,

$$q_{gc} = 1.05 \times 10^4 k(T_2 - 300) \text{ watts} , \quad (6)$$

where k, thermal conductivity,<sup>1</sup> is obtained from Fig. 2, at the average temperature,  $\bar{T} = 1/2(T_1 + T_2)$ .

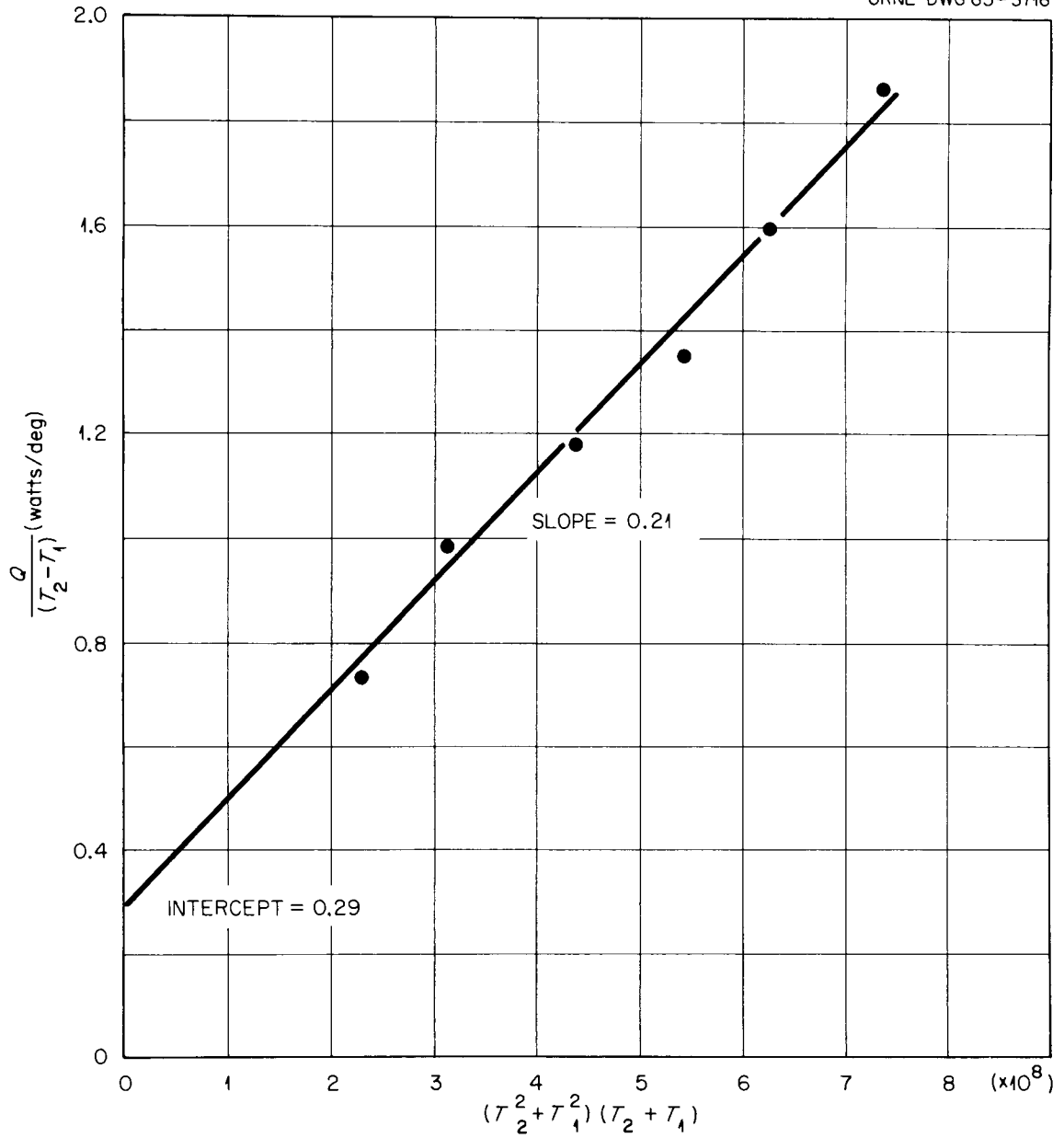


Fig. 1. Evaluation of the Constants A and B in the Equation,  $Q = A(T_2 - T_1) + B(T_2^4 - T_1^4)$ .

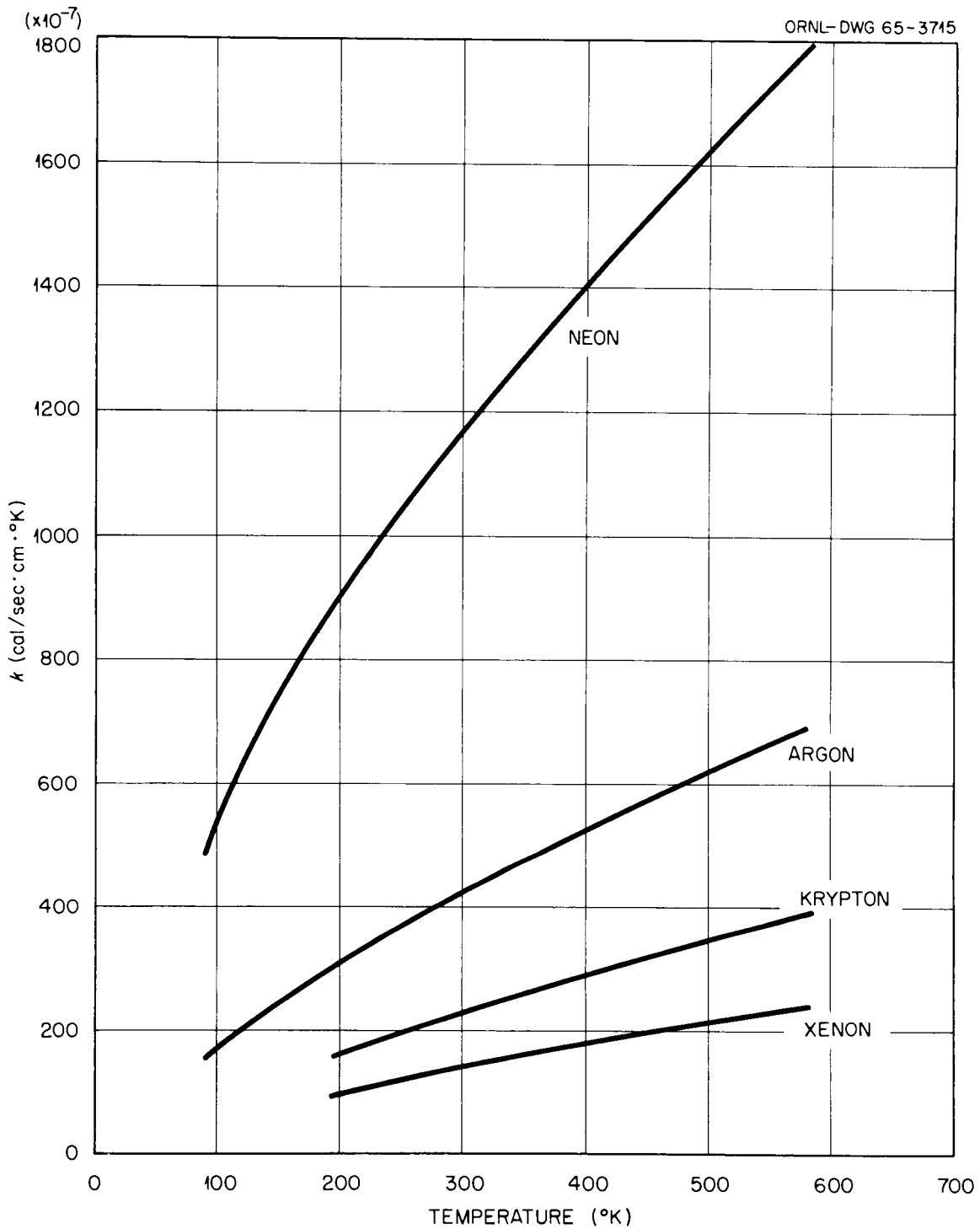


Fig. 2. Thermal Conductivity of the Inert Gases as a Function of Temperature.

Values for heat loss via radiation ( $q_r$ ), direct conduction ( $q_{dc}$ ), and gas conduction ( $q_{gc}$ ) were calculated at various heater temperatures and a cold wall temperature of 300°K from Eqs. 3, 4, and 6 and are shown in Fig. 3.

A test column was filled with neon to a pressure of 5 psig and data were taken of power input and heater sheath temperature. The difference between these values of power input and the heat transferred by radiation, direct conduction, and gas conduction was attributed to heat transfer by convection,  $q_c = Q - (q_r + q_{dc} + q_{gc})$ . The total power input and the heat transferred by convection are also shown in Fig. 3 as a function of heater temperature.

From these curves the fractions of heat dissipated by gas conduction, radiation, direct conduction, and convection were calculated and plotted as functions of heater power input as shown in Fig. 4. Since radiant heat loss is strongly affected by the surface condition of both the heater and the cold tube, and direct conductive heat loss is influenced by the mechanical pressure between the heater and the spacers, this representation can be regarded as typical but not exact for similar columns.

#### Pressure at Maximum Separation

When the gas pressure in a thermal diffusion column is adjusted to achieve maximum separation, the coefficient of convective remixing,  $K_c$ , is equal to the coefficient of diffusive remixing,  $K_d$ , given by Eqs. 7 and 8,

$$K_c = (\rho^4/\eta^3)r_1^8k_c, \quad (7)$$

$$K_d = \eta r_1^2k_d, \quad (8)$$

where

$$\begin{aligned} r_1 &= \text{cold tube radius, cm,} \\ \rho &= \text{average gas density, g/cm}^3, \\ \eta &= \text{average gas viscosity, poise, and} \\ k_c \text{ and } k_d &= \text{temperature and geometrical correction factors.} \end{aligned}$$

If  $K_c$  is set equal to  $K_d$ , then  $\eta^4k_d = r_1^6\rho^4k_c$  is obtained.

For the standard columns used (0.440-in. heater dia and 0.688-in. cold tube i.d.),  $r_1 = 0.874$  cm,  $k_d = 2.62$ , and  $\bar{T} = 1/2(T_2 + 300)$  °K. The other terms are functions of temperature and may be expressed as Eqs. 9, 10, and 11,

$$\eta = \eta_0(\bar{T}/273)^n, \quad (9)$$

$$\rho = \rho_0 P(273/\bar{T}), \quad (10)$$

$$k_c = 0.0066(T_2/T_1 - 1.3), \quad (11)$$

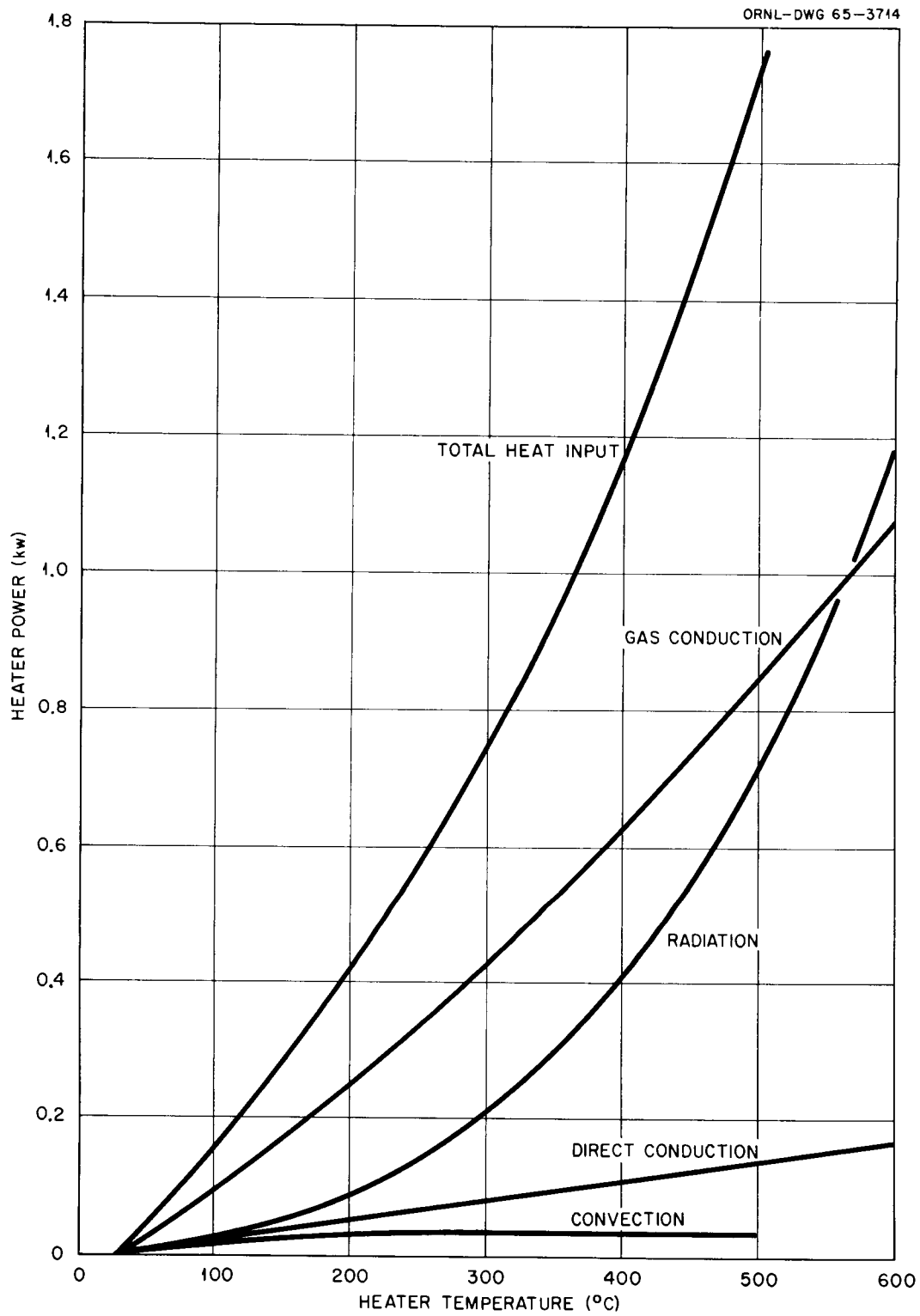


Fig. 3. Heat Transfer of Neon in a 0.75-in. by 7-ft Thermal Diffusion Column.

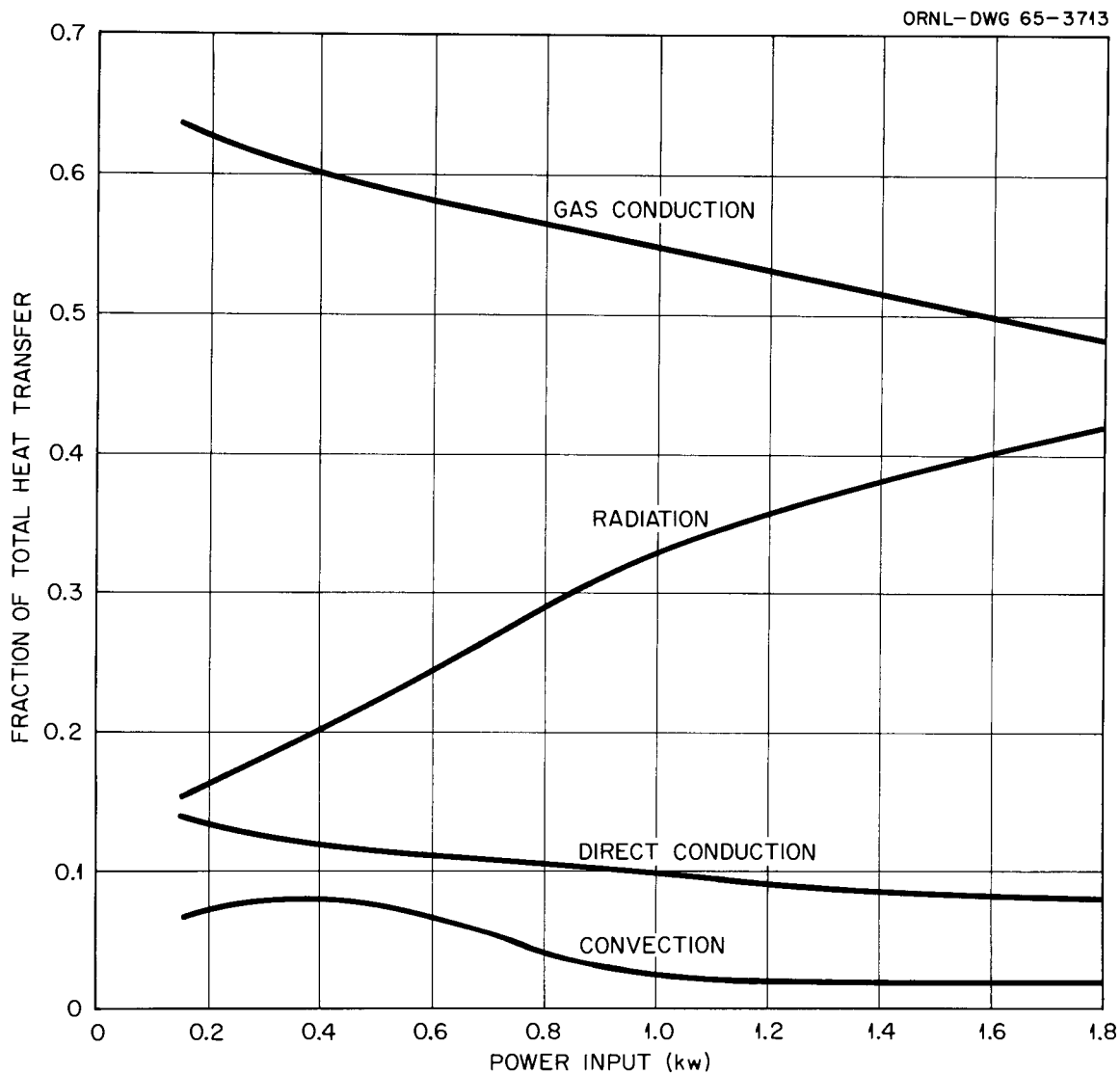


Fig. 4. Fractions of Total Heat Transferred by Various Means at Different Power Inputs.

where

P = pressure,  
 $\eta_0$  = viscosity at standard conditions,  
 $\rho_0$  = density at standard conditions, and  
 n = correction factor which varies with temperature.

If these terms are inserted into the expression equating  $K_c$  and  $K_d$ , the pressure at maximum separation can be obtained using Eq. 12,

$$P = \frac{22.7(\eta_0/\rho_0)}{(T_2 - 390)^{0.25}} \left( \frac{T_2 + 300}{546} \right)^{(1 + n)} \quad (12)$$

The log of pressure, P, at maximum separation is plotted as a function of heater temperature,  $T_2$ , in Fig. 5 for neon, argon, krypton, and xenon. When the separation factor versus gas pressure of a given gas in a standard column is plotted (Fig. 6), the actual heater temperature in the column can be estimated from Fig. 5 from the pressure corresponding to the maximum separation factor.

#### Separation Factor Relationships

The separation factor per unit mass,  $q^*$ , is given by Eq. 13,

$$\ln q^* = \frac{H^*L}{K_c + K_p + K_d} \quad (13)$$

where

$H^*$  = coefficient of thermal diffusion transport per unit mass,  
 L = length of column, and  
 $K_p$  = coefficient of parasitic convection.

The coefficient of parasitic remixing,  $K_p$ , arises due to unknown inaccuracies within the column such as nonuniform surface temperature distribution and imperfect centering of the heater.

The coefficient of thermal diffusion transport, H, is given by Eq. 14,

$$H = \frac{m_2 - m_1}{m_2 + m_1} (1 - n)(\rho^2/\eta)r_1^4h \quad (14)$$

or per unit mass by Eq. 15,

$$H^* = \frac{1 - n}{2M} (\rho^2/\eta)r_1^4h \quad (15)$$

where

h = temperature and geometrical correction factor,  
 $m_1$  and  $m_2$  = masses of molecules of species 1 and 2, and  
 M = molecular weight.

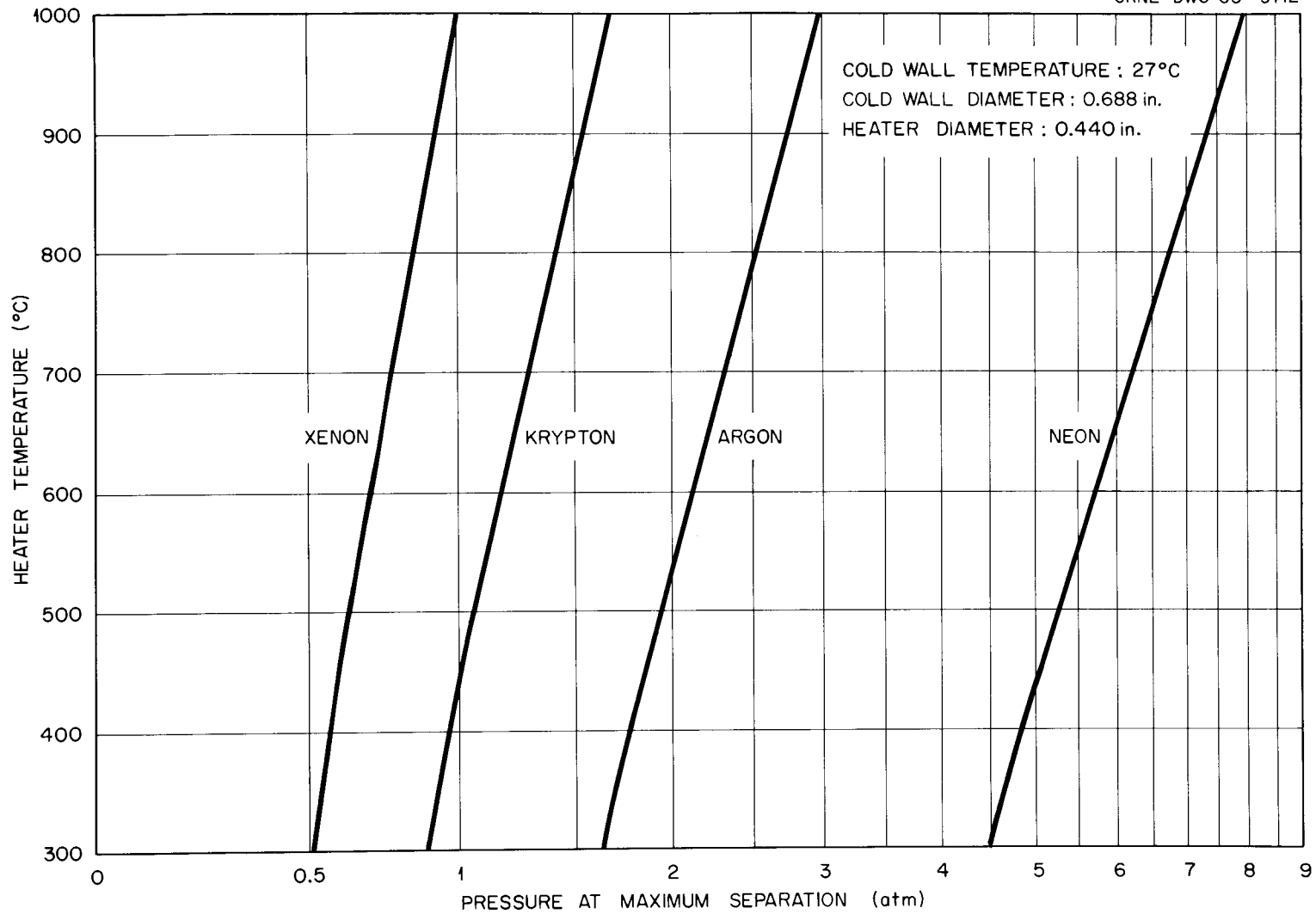


Fig. 5. Effective Heater Temperature Determined by Pressure at Maximum Separation.

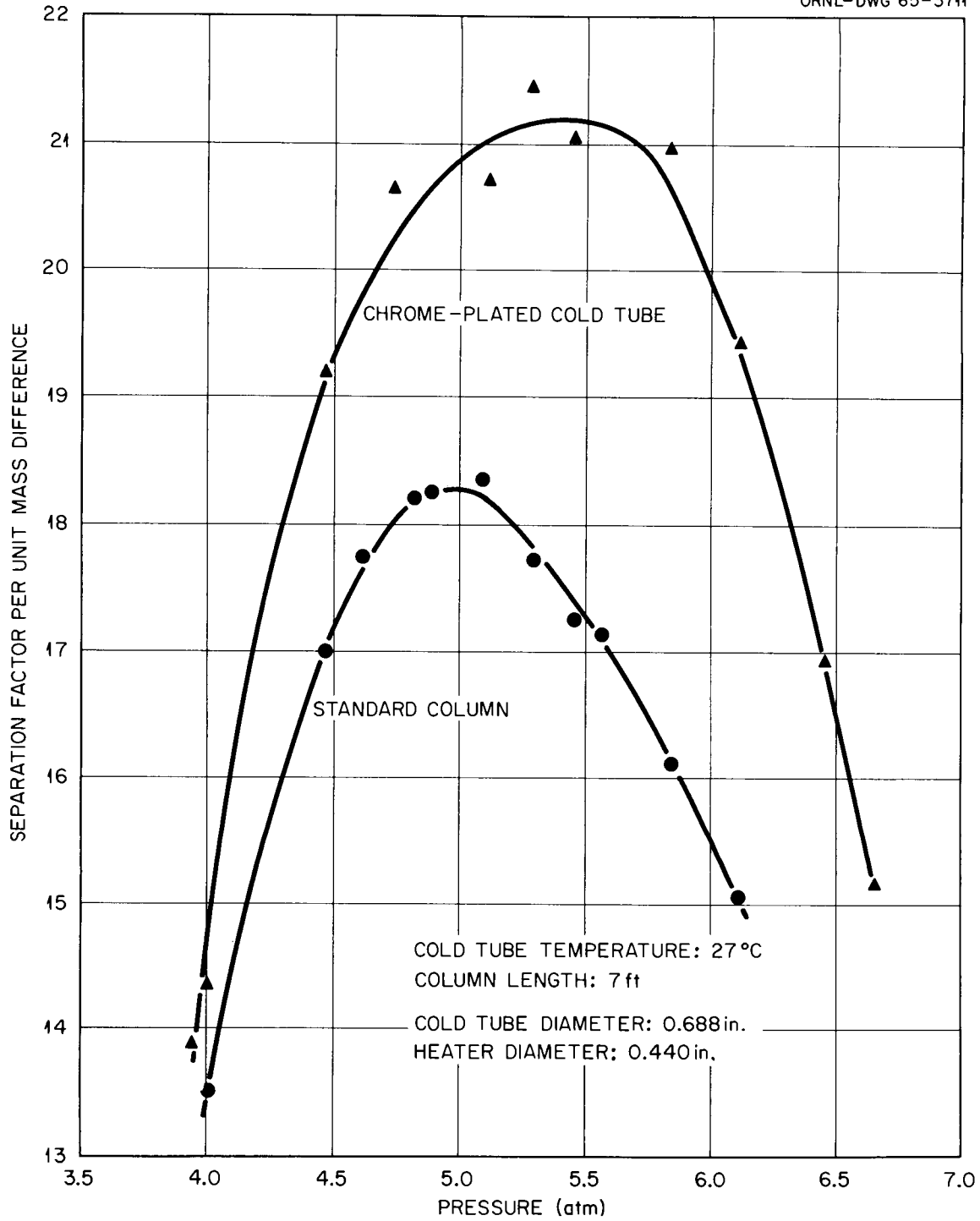


Fig. 6. Separation Factor of Neon as a Function of Pressure.

For standard columns used in this laboratory operating with 27°C cooling water,  $r_1 = 0.874$  cm,  $T_1 = 300^\circ\text{K}$ ,  $h = 0.347(T_2/T_1 - 1.3)$ ,  $k_c = 0.0066(T_2/T_1 - 1.3)$ , and  $k_d = 2.62$ . When these values and Eqs. 9 and 10 are inserted in the equations for  $H^*$ ,  $K_c$ , and  $K_d$ , then Eqs. 16, 17, and 18 are obtained,

$$H^* = 3.37 \times 10^{-4} \left( \frac{1-n}{M} \right) (\rho_0^2/\eta_0) P^2 \left( \frac{546}{T_2 + 300} \right)^{(2+n)} (T_2 - 390), \quad (16)$$

$$K_c = 7.47 \times 10^{-6} (\rho_0^4/\eta_0^3) P^4 \left( \frac{546}{T_2 + 300} \right)^{(4+3n)} (T_2 - 390), \quad (17)$$

$$K_d = 2\eta_0 \left( \frac{T_2 + 300}{546} \right)^n. \quad (18)$$

If neon isotopes are to be separated, then  $M = 20.18$  g/mole,  $n = 0.64$ ,  $\rho_0 = 0.9 \times 10^{-3}$  g/cm<sup>3</sup>, and  $\eta_0 = 315 \times 10^{-6}$  poise and Eqs. 19 through 21 are obtained for a standard column with heater temperature,  $T_2$ , and gas pressure,  $P$ ,

$$H^* = 0.26 P^2 \left( \frac{T_2 - 390}{T_2 + 300} \right)^{2.64}, \quad (19)$$

$$K_c = 2.44 \times 10^9 P^4 \left( \frac{T_2 - 390}{T_2 + 300} \right)^{5.92}, \quad (20)$$

$$K_d = 1.12 \times 10^{-5} (T_2 + 300)^{0.64}. \quad (21)$$

The temperature of the standard column used to obtain the data shown in Fig. 6 was not measured directly, but measurements made on an identical column showed that for the power input used (1.98 kw) a temperature of 530°C could be expected. Thus if  $T_2 = 803^\circ\text{K}$  and the maximum separation factor occurred at 4.95 atm,  $H^* = 2.40 \times 10^{-5}$  g/sec,  $K_c = 5.90 \times 10^{-4}$  g/cm.se and  $K_d = 9.98 \times 10^{-4}$  g/cm.sec.

If the ratio,  $R$ , equals  $K_p/K_c$  then, at the maximum separation factor,  $K_d = K_c(1 + R)$ , and from this  $R = 0.69$  and  $K_p = 4.07 \times 10^{-4}$  g/cm.sec.

The effective heater length of the standard column is 7 ft (213 cm) and the maximum separation factor from Fig. 6 is 18.3. Using Eq. 13,  $K_c$ ,  $K_d$ , and the previous values,  $H^* = 2.73 \times 10^{-5}$  g/sec which compares with the theoretical value of  $H^* = 2.40 \times 10^{-5}$  g/sec.

The second curve shown on Fig. 6 was obtained from data taken on an identical column except that the inside of the cold tube was chrome-plated in an attempt to conserve radiant heat and increase the temperature of the

heater for a given power input. The maximum separation factor occurs at a pressure of  $\sim 5.4$  atm, and the theoretical values of  $H^*$ ,  $K_C$ , and  $K_d$  at this point are given by Eqs. 22 through 24,

$$H^* = 7.61 \left( \frac{T_2 - 390}{T_2 + 300} \right)^{2.64}, \quad (22)$$

$$K_C = 2.14 \times 10^{12} \left( \frac{T_2 - 390}{T_2 + 300} \right)^{5.92}, \quad (23)$$

$$K_d = 1.12 \times 10^{-5} (T_2 + 300)^{0.64}. \quad (24)$$

For the standard column, the value of  $H^*$  calculated from the observed separation factor agrees fairly well with the theoretical value at the point of maximum separation factor. Since the  $\ln q^* \cong H^*L/2K_d$ , by using Eqs. 22 and 24 the temperature for the heater in the chrome-plated column was calculated as  $T_2 = 586^\circ\text{C} = 859^\circ\text{K}$  or about  $56^\circ$  higher than the temperature of the standard column.

Using this value,  $T_2 = 859^\circ\text{K}$ , and the same equations that were applied to the standard column, values were calculated for  $H^*$ ,  $K_C$ ,  $K_d$ , and  $K_p$ ,

$$H^* = 2.90 \times 10^{-5} \text{ g/sec},$$

$$K_C = 7.29 \times 10^{-4} \text{ g/cm.sec},$$

$$K_d = 1.01 \times 10^{-3} \text{ g/cm.sec},$$

$$K_p = 2.83 \times 10^{-4} \text{ g/cm.sec},$$

at the pressure where the separation factor is a maximum.

#### Preenrichment of Feed Material

Normal neon containing 0.26%  $^{21}\text{Ne}$  was used as the feed material for enriching the middle neon isotope —  $^{21}\text{Ne}$ . The effect on final concentration of using feed material preenriched in  $^{21}\text{Ne}$  was studied. A computer program was written to make a material balance of all components in a column at equilibrium and to calculate the concentration distribution as a function of column length.

The total length of the system was 10 columns, each 15 ft long, connected in series; four different feed concentrations were assumed as follows:

<u><math>^{20}\text{Ne}</math>, %</u>	<u><math>^{21}\text{Ne}</math>, %</u>	<u><math>^{22}\text{Ne}</math>, %</u>	
90.8	0.26	8.9	(Normal)
49.5	1.00	49.5	
49.0	2.00	49.0	
47.5	5.00	47.5	

The computed results of filling a system 150 ft long with each of these materials and allowing the system to come to equilibrium are shown in Fig. 7. Since this figure shows that the peaks for pre-enriched  $^{21}\text{Ne}$  are considerably higher than the peak for normal neon, the feasibility of constructing a system to produce enriched  $^{21}\text{Ne}$  feed material was studied. A preliminary design indicates that two 7.5-ft columns in series, fed with normal neon at the center connection, with enriched  $^{20}\text{Ne}$  rejected at the top, should produce material assaying 49.2%  $^{20}\text{Ne}$ , 1.6%  $^{21}\text{Ne}$ , and 49.2%  $^{22}\text{Ne}$  at the bottom of the system.

The peak concentrations indicated on Fig. 7 can be increased to higher values in a batch operation by removing the depleted material in the two or three columns at each end and refilling with enriched  $^{21}\text{Ne}$  feed.

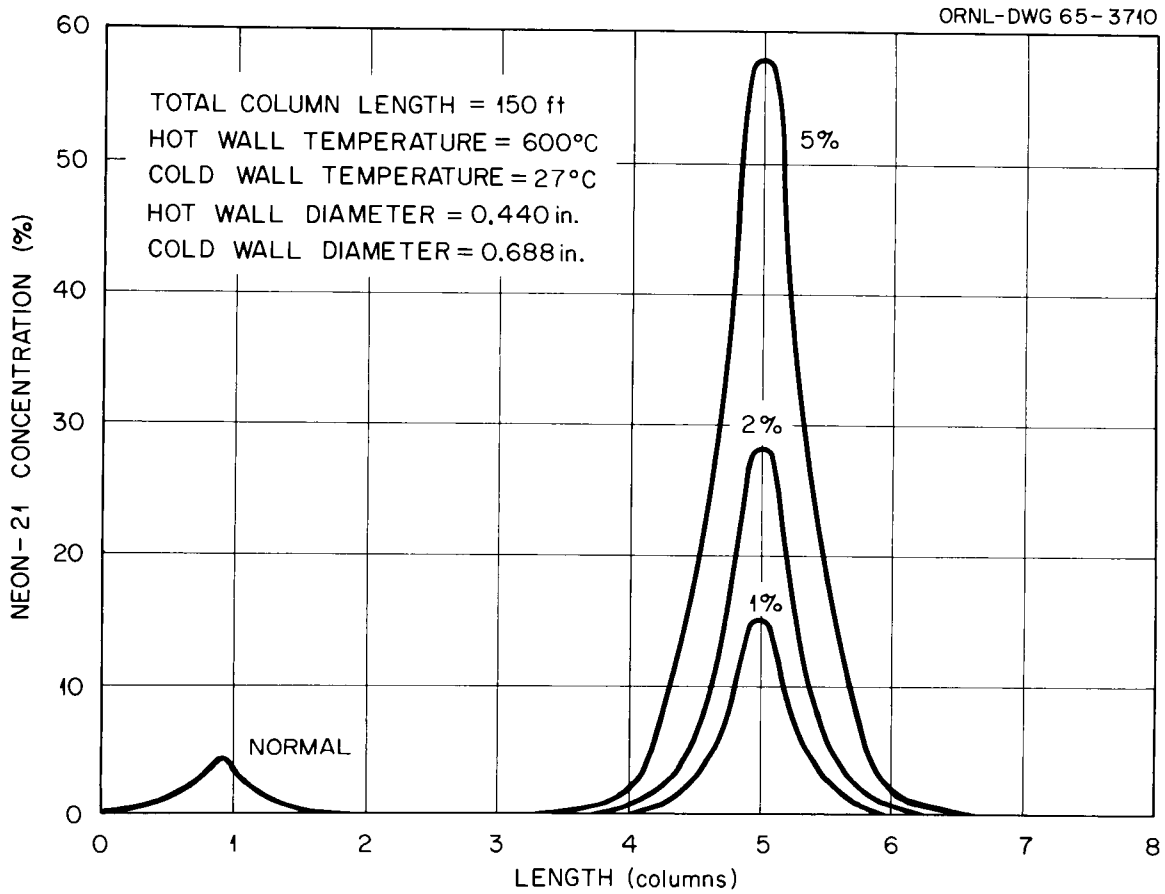


Fig. 7. Neon-21 Concentration at Equilibrium for Various Feed Material Concentrations as a Function of Column Length.

## OPERATIONS AND PRODUCT ENRICHMENTS

Neon

Data for the curve in Fig. 8, which can be used to estimate the amount of time required to reach specific  $^{21}\text{Ne}$  enrichment levels, were obtained by simultaneously assaying samples from several points spaced unit-column lengths apart and plotting the percent of  $^{21}\text{Ne}$  with respect to  $^{20}\text{Ne}$  or  $^{22}\text{Ne}$  (and disregarding the third isotope since it is present in minute amounts at either end of the thermal diffusion system). As  $^{20}\text{Ne}$  or  $^{22}\text{Ne}$  was removed from the system, the  $^{21}\text{Ne}$  peak and the isotopic distribution were shifted in the column. The rate of increase or decrease in the enrichment of  $^{21}\text{Ne}$  can be determined from the slope of the curve.

The curve is assumed to be symmetrical about the 50% position when the third isotope is disregarded. When three isotopes are considered, the curve is rounded over the middle isotope peak because the third isotope becomes appreciable in the center of the system. In Fig. 8, if the sharp peak were not rounded, the amount of  $^{21}\text{Ne}$  would be  $\sim 37.5\%$  instead of  $35\%$ . The dotted side of the  $^{21}\text{Ne}$  peak is obtained from the assumption that the  $^{22}\text{Ne}-^{21}\text{Ne}$  intermolecular forces at one end of the system are similar to the  $^{20}\text{Ne}-^{21}\text{Ne}$  intermolecular forces at the other end of the system, so that the peak is essentially symmetrical.

The theoretical curve is based on calculations made using optimum estimated values for column parameters and the theoretical equations of Jones and Furry<sup>2</sup> and Rathkamp.<sup>3</sup> The experimental curve closely approximates that of a theoretical column 80% of the length of the existing columns. The area shown by diagonal hatching represents the amount of 100%  $^{21}\text{Ne}$  that must be put into the system to obtain the indicated peak. The length of time necessary to increase  $^{21}\text{Ne}$  enrichments from one level to another (Table 1) can be estimated from the rate at which  $^{20}\text{Ne}$  was withdrawn ( $\sim 14$  liters/week), the rate that  $^{22}\text{Ne}$  was withdrawn ( $\sim 6$  liters/month), the rate that normal neon was added to the system (0.26% in  $^{21}\text{Ne}$  which is equivalent to  $\sim 40$  ml/week of 100%  $^{21}\text{Ne}$ ), and the area of the  $^{21}\text{Ne}$  peak from the graph.

Table 1. Time required to increase neon-21 enrichment

Enrichment, %		Time required, days
Beginning	Ending	
20	30	29
30	40	31
40	50	39
50	60	48
60	70	57
70	80	87
80	92	150

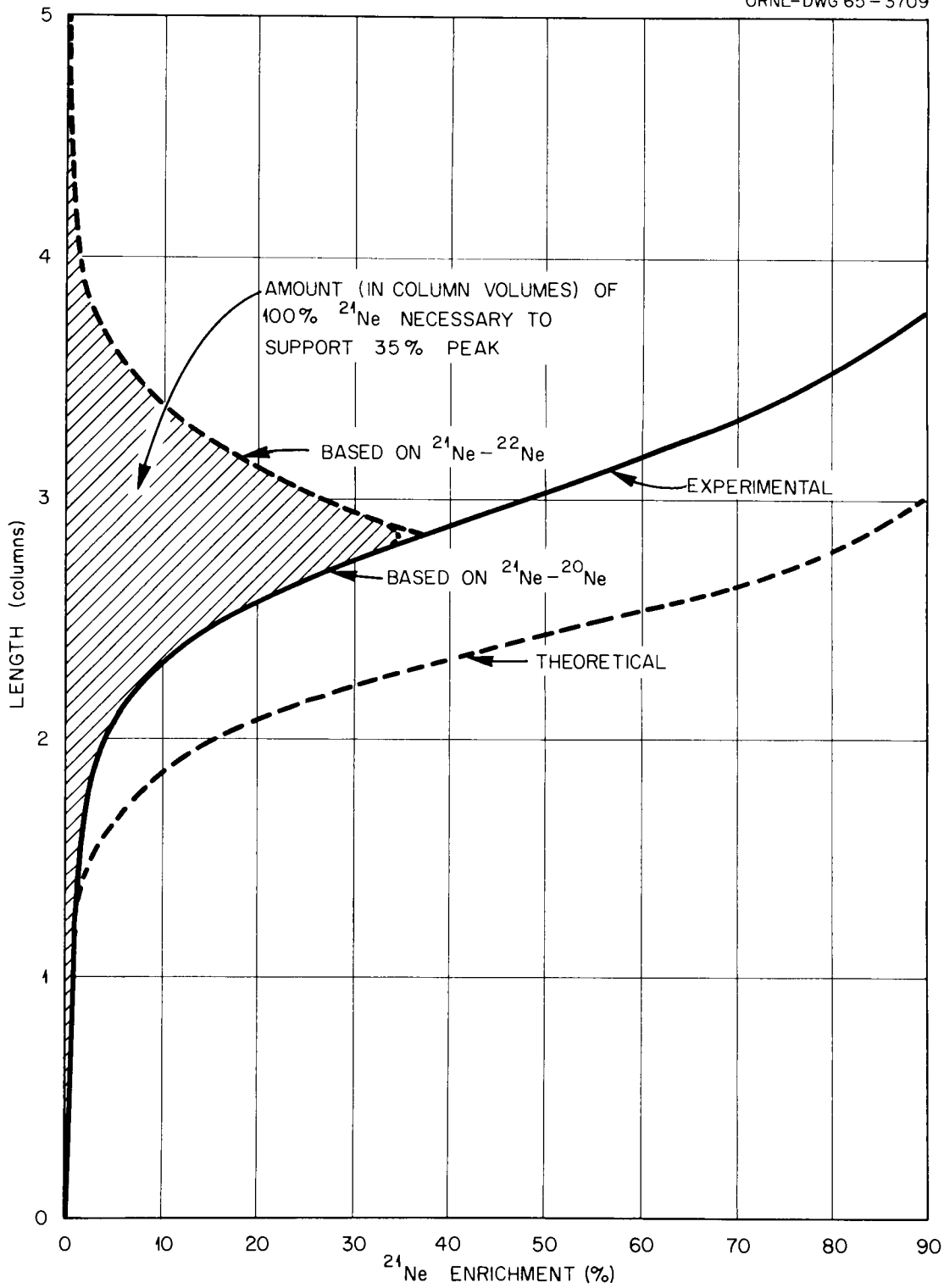


Fig. 8. Neon-21 Enrichment as a Function of Column Length.

Actual enrichments obtained during the first half of the year were equivalent to these estimates when allowances are made for down-time of equipment.

At the beginning of the year, the neon system was arranged with ten 15-ft concentric tube columns connected in series<sup>4</sup> with a 2-liter volume at the bottom for accumulation of <sup>22</sup>Ne, a 5-liter volume at the top for <sup>20</sup>Ne, a 250-ml volume three columns from the bottom for <sup>21</sup>Ne, and a double-ended bellows pump connected across the ends of the system to facilitate inter-column gas mixing. During the first five months, ~109 liters of 99.99% <sup>20</sup>Ne containing <0.1% H<sub>2</sub> was released to inventory and ~6.4 liters of 99.8% <sup>22</sup>Ne was removed to in-process inventory. In May, 260 ml of 30.15% <sup>21</sup>Ne was removed from the middle volume and released to inventory. The system developed leaks during June and the buildup of <sup>21</sup>Ne had to start anew. The progress in <sup>21</sup>Ne enrichment from July to December is shown in Table 2 which gives percent of <sup>21</sup>Ne taken from various points in the system. A <sup>21</sup>Ne enrichment of 51.2% was reached during December.

Table 2. Enrichment of neon-21  
July-December 1964

Date	Position, columns from bottom	Neon-21, %
July 20	4	9.0
August 17	2	16.1
August 27	3	16.1
September 23	3	23.1
October 26	3	37.3
November 30	3	43.7
December 21	3	51.2

The comparison of enriched neon (51.2% <sup>21</sup>Ne) and normal neon with a natural abundance of 0.26% <sup>21</sup>Ne is given in Fig. 9.

The buildup rate increased ~50% during the last half of the year due to the removal of <sup>20</sup>Ne at an enrichment of >99.9%, relocation of the feed-in point for starting material (after removal of <sup>20</sup>Ne or <sup>22</sup>Ne) down to the center of the system, and removal of the center volume which released material necessary to sustain a gradient between <sup>21</sup>Ne and adjacent isotopes.

#### Argon

At the first of the year the argon system operated with all columns (20 columns 7 ft in length and 3 columns 15 ft in length) connected in series. These were concentric tube columns with annuli of ~1/4 in.<sup>2</sup>. An effort was made to remove <sup>38</sup>Ar at an enrichment of ≥20%; ~220 ml of 20% material had been removed in December 1963.

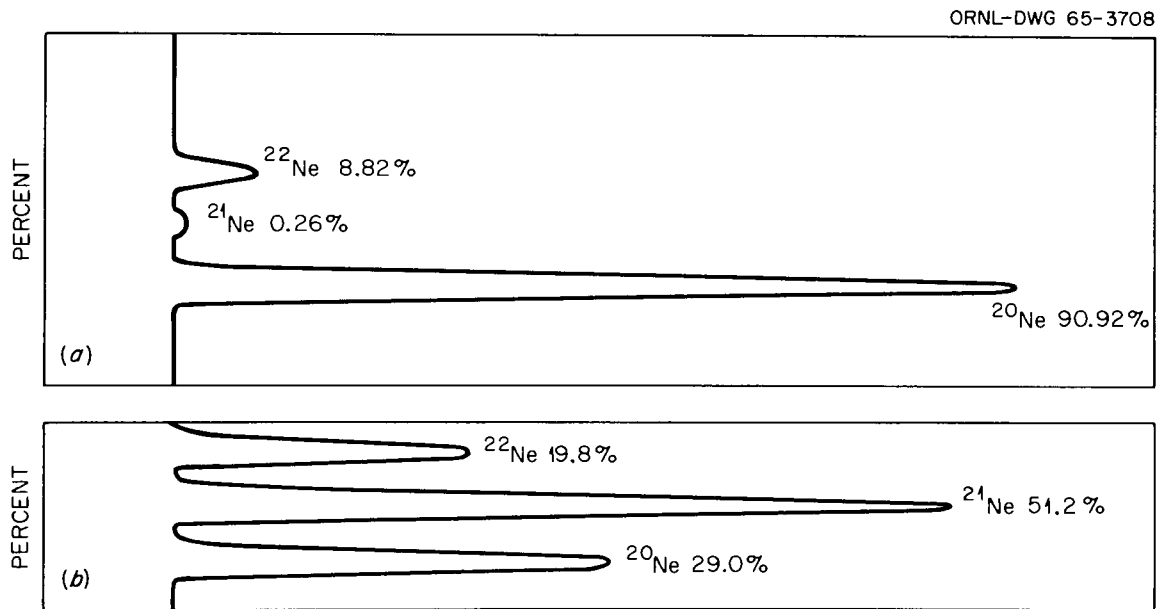


Fig. 9. a. Mass Spectrum of Normal Neon with Neon-21 on a Scale Ten Times More Sensitive Than That of Neon-20 and Neon-22.

b. Mass Spectrum of Neon Enriched in Neon-21. All peaks on same sensitivity scale.

In January, 30 ml of 20.0%  $^{38}\text{Ar}$  with a chemical purity of 99.9% was moved to production inventory. At the beginning of the year, the  $^{38}\text{Ar}$  enrichment, seven short-column lengths (~50 ft) from the top of the system, was 18.9%. Assays during February showed no increase in enrichment; therefore, a system for pre-enriching  $^{38}\text{Ar}$  was installed. It consisted of two 3-1/2-ft columns and one 7-ft column; the shorter parallel columns were connected in series with the 7-ft column. The columns contained calrod heaters 0.351 in. in dia placed in 3/4-in. copper water-cooled tubes, making annuli of ~3/16 in. The system operated at a pressure of 1-2 psi greater than the regular argon system. An enrichment of ~1.3%  $^{36}\text{Ar}$  and ~0.13-0.15%  $^{38}\text{Ar}$  at a rate of 11 ml/hr was obtained when an excessive feed rate through a manifold connected across the bottom of the two parallel columns simulating an infinite end-volume was used. The problem of controlling the feed rate was solved by replacing the conventional feed valves (leak-in via needle valve) with electrically operated valves timed to allow a known volume of gas to enter or leave the system. With these valves, the feed rate was varied over wide limits (2.5-45 ml/hr) with very little change in output enrichment (increasing from 0.123%  $^{38}\text{Ar}$  to 0.126%). This output was fed back into the regular argon system at a point where the  $^{38}\text{Ar}$  assay nearly matched that of the system. This arrangement, however, did not improve  $^{38}\text{Ar}$  enrichment.

In March, the original method of operation was resumed: 10 short columns in parallel in the first stage, 2 long columns in parallel in the second stage, topped by 1 long column and 10 short columns in series. Still, very little improvement was noted. In May, addition and withdrawal rates of feed at the bottom of the system were increased. Improvement in operation allowed the removal of light-end impurities and later 927 ml of ~99%  $^{36}\text{Ar}$  which was transferred to production inventory.

Due to faulty calrod heaters, the  $^{38}\text{Ar}$  enrichment fell during the period from June to December. In December, the  $^{38}\text{Ar}$  enrichment was five columns from the top at 4.6%. Several 15-ft columns are being fabricated to increase the length without decreasing the width of the system by using columns from the bottom parallel group. The results of the  $^{21}\text{Ne}$  enrichment system have encouraged a similar arrangement of the argon system. The low natural abundance of  $^{38}\text{Ar}$  (0.06%) as compared with the natural abundance of  $^{21}\text{Ne}$  (0.26%) necessitates, however, a longer system (while still, perhaps, wider at the bottom) for enrichment of the middle isotope.

### Krypton

The krypton system began operation in May 1963 to enhance both the light and heavy ends of krypton. All concentric tube columns with annuli of 1/8 in. were connected in series with a double-ended bellows pump attached across the ends of the system.<sup>4</sup> In December 1963, the bellows pump stopped working due to the shaft slipping on the driving gear. The heavy-isotope compartment of the bellows pump held ~300 ml of 81.2%  $^{86}\text{Kr}$ . (The natural abundance of  $^{86}\text{Kr}$  is 17.37%.) The maximum  $^{86}\text{Kr}$  enrichment at the bottom of the system during each month is shown in Fig. 10.

ORNL-DWG 65-3707

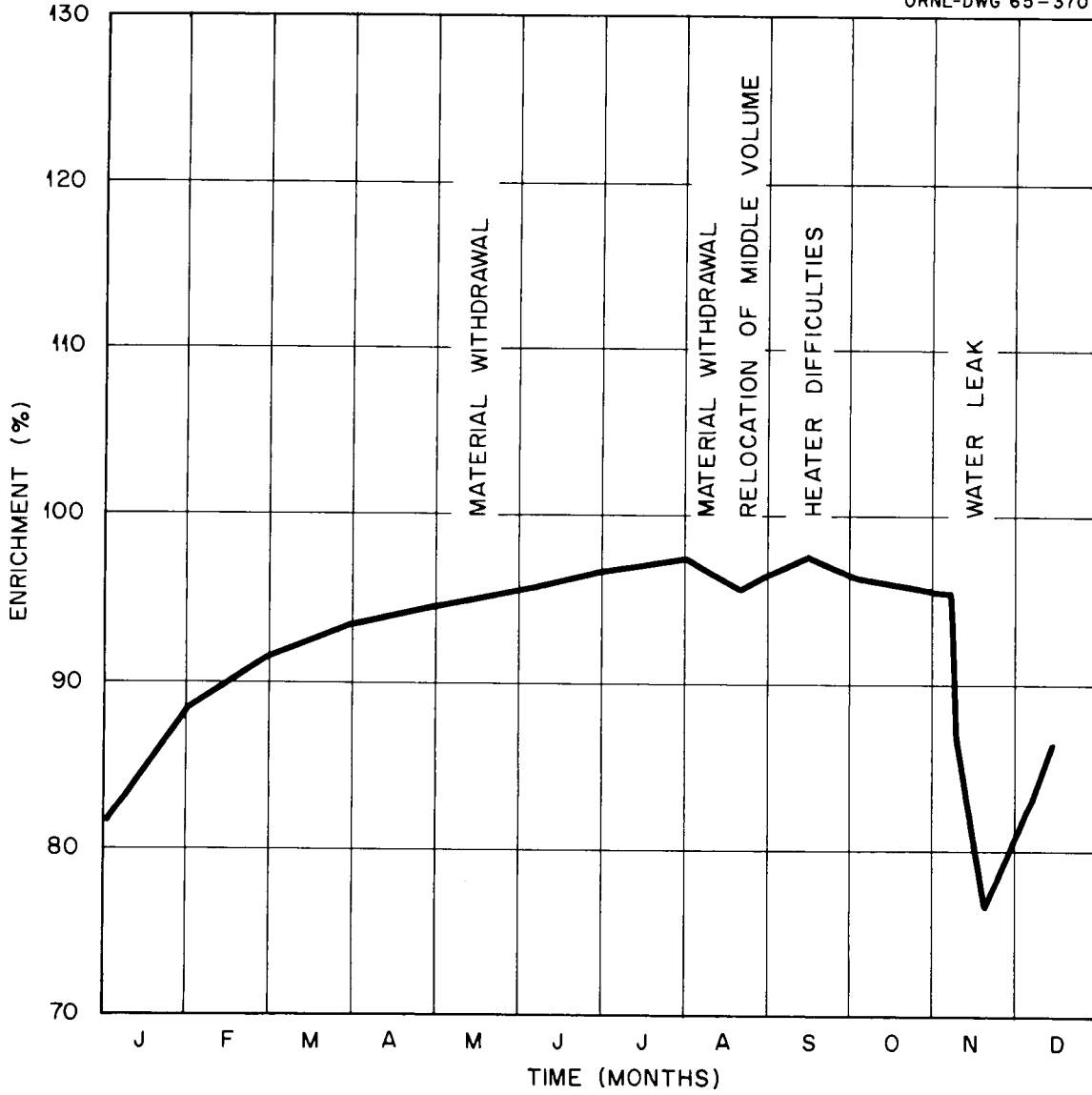


Fig. 10. Krypton-86 Enrichment During January-December 1964.

In February, 10 ml of 88.3%  $^{86}\text{Kr}$  was removed along with 30 ml of light-end impurities ( $\text{H}_2$ ,  $\text{N}_2$ , etc.). In March, 91 ml of 92-93%  $^{86}\text{Kr}$  was removed with light-end isotopes assaying  $\sim 7.4\%$   $^{78}\text{Kr}$  and  $\sim 26\%$   $^{80}\text{Kr}$  with still much  $\text{N}_2$  and  $\text{H}_2$ . (The natural abundance of  $^{78}\text{Kr}$  is 0.35% and that of  $^{80}\text{Kr}$  is 2.27%.)

In April, 50 ml of 4.16%  $^{78}\text{Kr}$  was removed containing 25.94%  $^{80}\text{Kr}$ . This material was removed one column from the top of the system, since the top was mostly  $\text{H}_2$  and  $\text{N}_2$ . In June, a light-end assay showed 7.17%  $^{78}\text{Kr}$  and 30.3%  $^{80}\text{Kr}$ .

In August, due to the slow buildup of  $^{86}\text{Kr}$ , the middle volume was moved up three columns to eleven columns from the bottom of the system; it had been at the center of the system. At the same time the depleted material was replaced from the center volume with normal material, and the pressure of the system was increased from 2 to 6 psig. The first dip in the graph in Fig. 10 shows this replacement and also the fairly quick recovery.

In September, 10 ml of 97.2%  $^{86}\text{Kr}$  was removed and in October  $\sim 4$  ml of 6.98%  $^{78}\text{Kr}$  was removed. Krypton-86 enrichment slowly fell and leveled off due to calrod heater difficulties in October. Defective heaters could be replaced only when operating conditions (or enrichment levels) permitted, since a long period of time is necessary to build up appreciable gradients. On October 21, the gas that was high in  $^{86}\text{Kr}$  was removed and all other gas was discarded; the system was shut down and all the defective heaters were replaced. The system was back in operation the next day.

In November, a leak suddenly occurred between the water cooling annulus and the gas annulus in the fifth column from the bottom of the system. Inspection of the system indicated that the heater had been shorted causing an excessive current through it. The column was immediately isolated from the rest of the system and then replaced, but not before water had entered the adjacent columns and spread throughout the entire system. The sharp dip during November in Fig. 10 is due to this leak. The less steep drop indicates the addition of more krypton. Most of the enriched  $^{86}\text{Kr}$  was recovered as seen by the rapid recovery in December when the  $^{86}\text{Kr}$  enrichment was 86.3% and still rising.

### Xenon

A system, consisting of 36 seven-ft long columns connected in series with a bellows displacement pump at each end, is in operation to enrich  $^{124}\text{Xe}$  whose natural abundance is 0.09%. The system has leveled off at a product concentration of  $\sim 3\%$   $^{124}\text{Xe}$ ; material will be withdrawn at this level before the end of the fiscal year.

### Product Enrichments

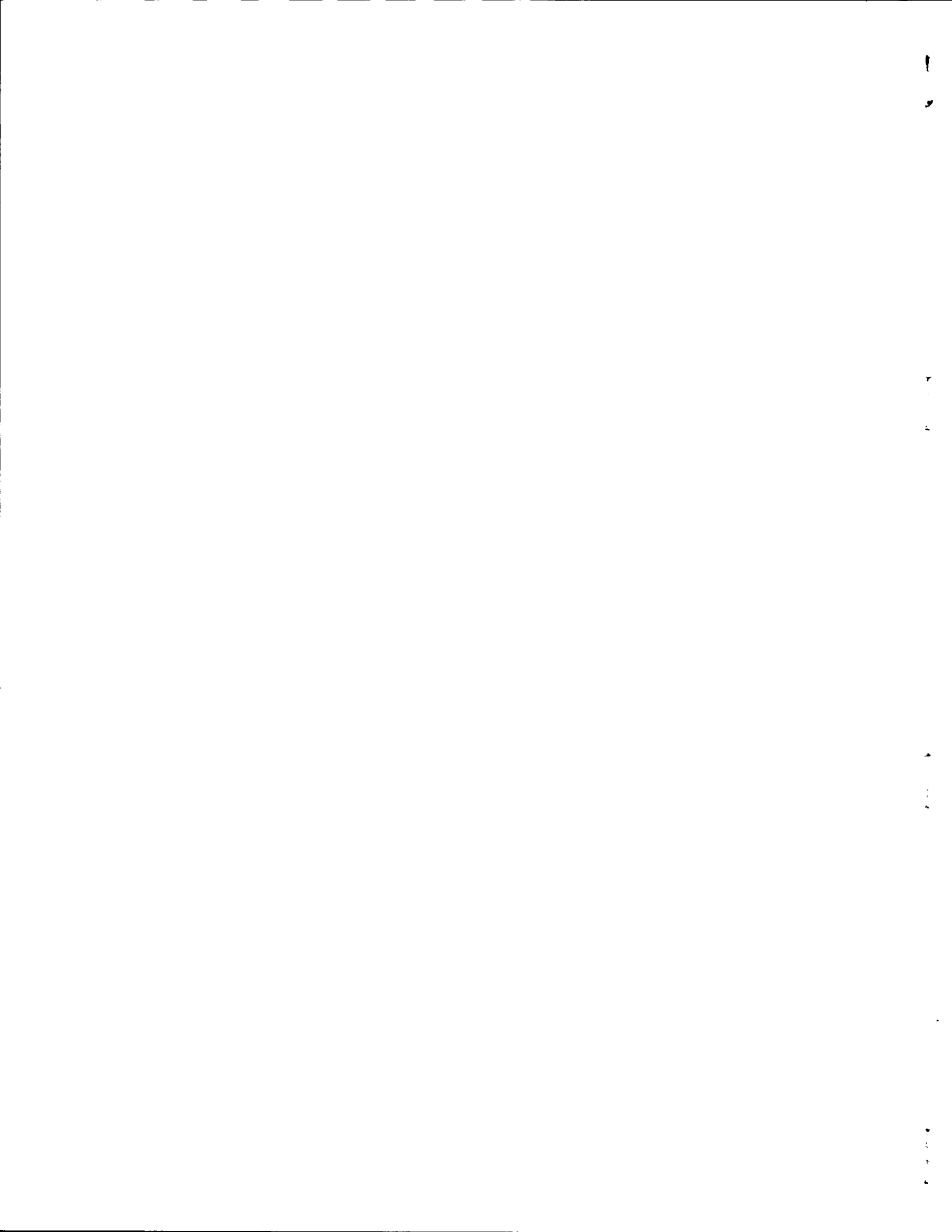
A summary of the amount and enrichment of isotopes obtained during 1964 can be seen in Table 3. Approximately 400 liters of  $^{20}\text{Ne}$  and  $\sim 65$  liters of  $^{22}\text{Ne}$ , held in in-process inventory temporarily, are not included in this list.

Table 3. Amount and enrichment of neon, argon, and krypton — January-December 1964

Isotope	Enrichment, %	Weight, mg
Neon-20	99.99	108,747
Neon-21	30.1	234
Neon-22	99.76	16
Argon-36	99.7	1,650
Argon-38	20.0	53
Krypton-78	4.2	185
Krypton-86	88—93	375
Krypton-86	95.6—97.2	311

## REFERENCES

1. R. D. Present, Kinetic Theory of Gases, McGraw-Hill Book Company, New York, 1958, p. 262.
2. R. C. Jones and W. H. Furry, The separation of isotopes by thermal diffusion, Revs. Modern Phys. 18(2): 151-224 (April 1946).
3. W. R. Rathkamp, Gaseous thermal diffusion at Oak Ridge National Laboratory (unpublished).
4. T. A. Butler, W. R. Rathkamp, and H. B. Greene, Review of ORNL thermal diffusion program, Jan.-Dec. 1963, USAEC Rpt. ORNL-3607, Oak Ridge National Laboratory (May 1964).



ORNL-3815  
 UC-22 - Isotope Separation  
 TID-4500 (41st ed.)

## INTERNAL DISTRIBUTION

- |                                     |                         |
|-------------------------------------|-------------------------|
| 1. Biology Library                  | 53. E. H. Kobisk        |
| 2-4. Central Research Library       | 54. R. H. Lafferty, Jr. |
| 5. Reactor Division Library         | 55. E. Lamb             |
| 6-7. ORNL - Y-12 Technical Library  | 56. L. Landau           |
| Document Reference Section          | 57. Ingrid Lane         |
| 8-27. Laboratory Records Department | 58. C. E. Larson        |
| 28. Laboratory Records, ORNL R.C.   | 59. R. S. Livingston    |
| 29. P. S. Baker                     | 60. L. O. Love          |
| 30. Russell Baldock                 | 61. H. G. MacPherson    |
| 31. E. E. Beauchamp                 | 62. R. E. McHenry       |
| 32. W. A. Bell                      | 63. M. Murray           |
| 33. S. Blumkin (K-25)               | 64. A. H. Narten        |
| 34. G. E. Boyd                      | 65. R. G. Niemeyer      |
| 35. T. A. Butler                    | 66. W. K. Prater        |
| 36. F. N. Case                      | 67. M. E. Ramsey        |
| 37. J. W. Cleland                   | 68. W. R. Rathkamp      |
| 38. T. F. Connolly                  | 69. S. A. Reynolds      |
| 39. J. A. Cox                       | 70. R. A. Robinson      |
| 40. F. L. Culler                    | 71. A. F. Rupp          |
| 41. J. S. Drury                     | 72. R. W. Schaich       |
| 42. D. E. Ferguson                  | 73. H. E. Seagren       |
| 43. J. L. Fowler                    | 74. M. J. Skinner       |
| 44. J. H. Gillette                  | 75. E. D. Shipley       |
| 45. W. M. Good                      | 76. A. H. Snell         |
| 46. H. B. Greene                    | 77. K. A. Spainhour     |
| 47. H. R. Gwinn                     | 78. E. H. Taylor        |
| 48. K. W. Haff                      | 79. D. B. Trauger       |
| 49. W. D. Harman                    | 80. F. Van der Valk     |
| 50. W. H. Jordan                    | 81. E. Von Halle (K-25) |
| 51. M. T. Kelley                    | 82. J. R. Walton        |
| 52. C. V. Ketron                    | 83. A. M. Weinberg      |
|                                     | 84. A. Zucker           |

## EXTERNAL DISTRIBUTION

85. P. C. Aebersold, Division of Isotopes Development, AEC, Washington, D.C.
86. Argonne National Laboratory, Lamont, Illinois
87. H. D. Bruner, Division of Biology and Medicine, AEC, Washington, D.C.
88. J. T. Cristy, AEC-RL00, Richland, Washington
89. D. C. Davis, Research and Development Division, AEC, ORO
90. D. R. de Boisblanc, Phillips Petroleum Company, Idaho Falls, Idaho
91. J. W. Irvine, 6-426, MIT, Cambridge, Massachusetts

92. T. R. Jones, Division of Research, AEC, Washington, D.C.
93. G. A. Kolstad, Division of Research, AEC, Washington, D.C.
94. P. W. McDaniel, Division of Research, AEC, Washington, D.C.
95. B. Manowitz, Brookhaven National Laboratory, Upton, Long Island, New York
96. J. W. Vanderryn, Atomic Energy Commission, Washington, D.C.
97. Research and Development Division, AEC, ORO
- 98-547. Given distribution as shown in TID-4500 (41st ed.) under Isotope Separation category (75 copies - CFSTI)